https://doi.org/10.26749/rstpp.103.17

PAPERS AND PROCEEDINGS OF THE ROYAL SOCIETY OF TASMANIA, VOLUME 103

THE MINERALOGY, PETROCHEMISTRY AND MAGMATIC HISTORY OF THE TAMAR LAVAS, NORTHERN TASMANIA

By

F. L. SUTHERLAND
Tasmanian Museum, Hobart

(With four text figures and two plates)

ABSTRACT

The Tertiary lavas of the Tamar Trough are mostly undersaturated to near-saturated alkali olivine-basalts, with minor flows of olivine-nephelinite, nepheline-basanite, limburgite and tholeiitic olivine-basalt.

Olivine forms the main phenocryst fraction in the lavas, but includes xenocrysts and late intergrowths, and ranges in composition from about Fo_{94} to Fo_{55}. Labradorite Ab_{38-41}, zoned to about Ab_{62}, is the typical feldspar. The clino-pyroxenes are augites, passing into titan-augite and aegirine-augite in the more alkaline rocks. Nepheline is represented in the olivine-nephelinites and basanite, and analcime is a late-stage accessory in the coarser olivine-basalts. The iron ore is ilmenite or titano-magnetite, commonly altered to leucoxene, and other accessory minerals include apatite, zeolites and biotite. The finer grained lavas tend to have glassy mesostases, darkened with iron ore in a few cases, and the coarser lavas commonly show microlitic, feldspathic and zeolitic mesostases.

Some of the lavas carry peridotitic xenoliths and xenocrysts, composed mostly of magnesian olivine, with some clino-pyroxene and spinel, and basalt at Corra Linn contains augite xenocrysts from depth, showing well developed reaction rims. Accidental xenoliths in the lavas include fused dolerite and sediments, in part replaced by clino-pyroxene.

Differentiation trends can be distinguished in the Tamar suite, both between separate lavas and within individual lavas. Differentiation within thick lavas of coarse basalt has produced picritic, mesostasis-rich and pegmatitic phases, and comparisons are made with differentiated rocks of similar compositions in sills and necks elsewhere in Australia.

The Tamar volcanic suite is predominantly an alkaline association, resembling the Older Volcanics of Victoria, the Auckland Basalts of New Zealand, and, to some extent, the Hawaiian alkali basalts.

The Tamar eruptions commenced about Upper Eocene time, with the initial alkali basalt magma ascending in a relatively undifferentiated state, before undergoing some differentiation prior to further eruption. Olivine-nephelinite then appears to have erupted, probably in the Oligocene and possibly during waning in the volcanism, before renewed and more wide-spread eruption of olivine-basalts in about Middle Tertiary time. Fractionation of augite, and possibly olivine, or spinel, at depth may have played a part in producing the magmas for these later lavas, with some low pressure differentiation giving the coarse olivine-basalts of the capping flows

The Tamar lavas form part of an alkaline volcanic association extending to the west, and pass transitionally into an olivine-tholeiite association to the east and south-east. The parent alkali basalt magmas possibly formed from relatively restricted partial mantle melting, with segregation of magma at depths of 35-70 Kms; olivine-tholeiite parent magmas on the south-eastern outskirts possibly formed from a greater degree of melting.

INTRODUCTION

Tertiary lavas outcrop along much of the Tamar Trough, a fault structure formed in or prior to the Palaeocene (Longman, 1966; Sutherland, 1966). This paper discusses the mineralogy, petrochemistry and magmatic history of these lavas, based on detailed geological and petrographic studies to be presented elsewhere; the petrography of the lavas is summarized here in a series of photomicrographic plates (Plates 1-12).

Numerous persons have assisted in the work as a whole, and more complete acknowledgment will be given elsewhere. However, the author would like to thank the following for assistance in aspects of this particular paper in regard to discussion, criticism and chemical data:—Dr R. Varne, Mr D McP. Duncan, Mr R. J. Ford, Mr M. R. Banks, and Mr C. Gee (Geology Department, University of Tasmania); Mr I. B. Jennings and Mr D. I. Groves (Tasmanian Department of Mines); Dr D. H. Green, Dr I. McDougall and Mr N. Gray, Department of Geology and Geophysics, Australian National University); Dr A. H. Spry (A.M.D.L., Adelaide, South Australia); and Mr P. Brumby, Mr F. Brown and Mrs G. Sanders. Mr W. Peterson (Geology Department, University of Tasmania) assisted with microslide photography, and Mr M. Bower (Tasmanian Museum) helped with preparation of rocks for analysis. This work represents part of an M.Sc. thesis submitted by the author to the University of Tasmania.

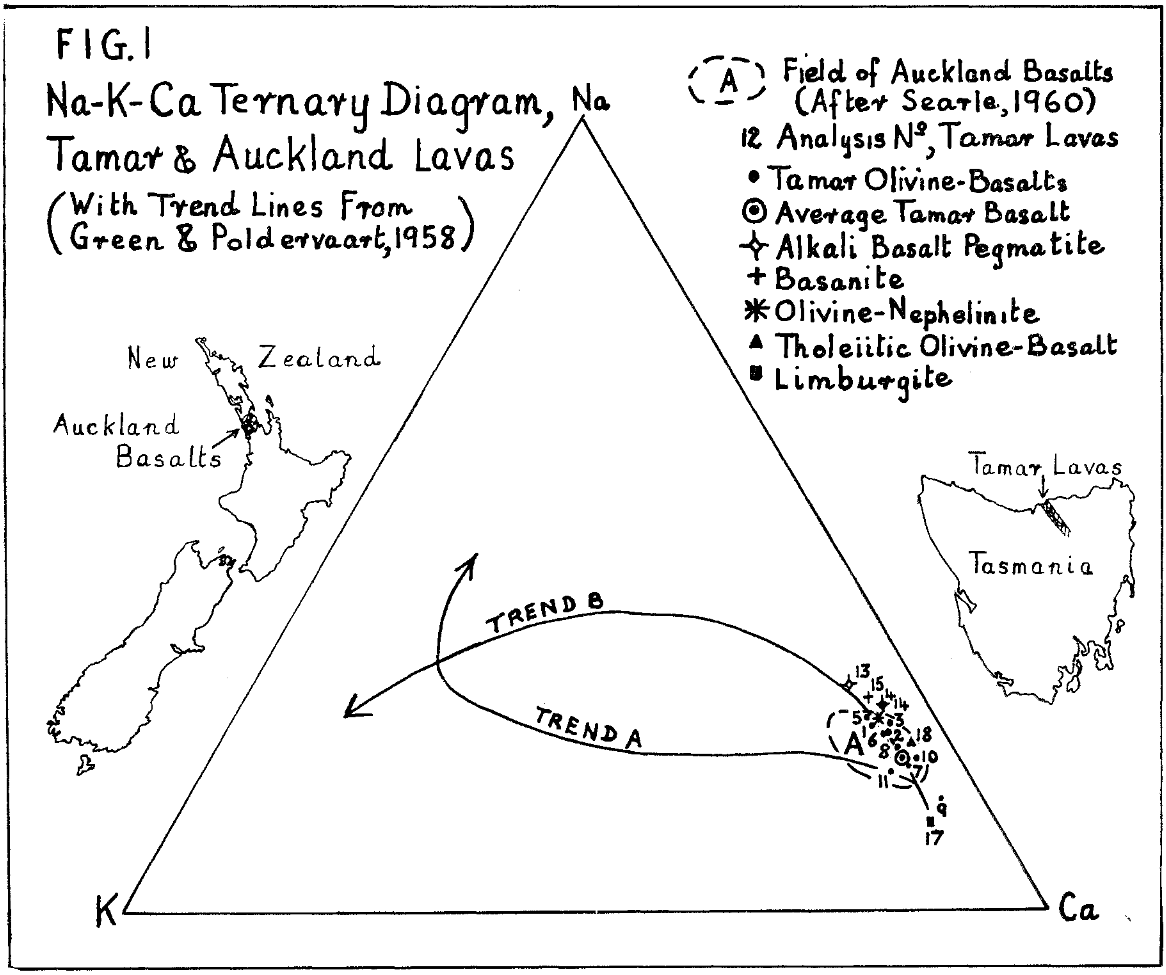

FIGURE 1—N.-K-Ca ternary chemical variation diagram of Tamar lavas, compared with the field of the Auckland basalts and the trend lines of Green and Poldervaart, 1958 (modified from Searle, 1960).

MINERALOGY AND ORDER OF CRYSTALLISATION IN THE TAMAR LAVAS

Determination of Mineral Compositions

Compositions of the main minerals crystallising in the Tamar lavas were gauged by the following methods:—Optic axial angles of olivines and pyroxenes were determined on a Leitz four-axis universal stage. Difficulties in determining olivine compositions from 2V measurement (Wyllie, 1959; Munro, 1966) are applicable to the data presented in this study, but numerous measurements were made and clearly aberrant values have been omitted; errors in the $2V_z$ values are probably not greater than ± 2°, corresponding up to about ± 4 mol. per cent of Mg_2SiO_4. Measurements of $2V_z$ of the clino-pyroxenes were corrected for refraction errors from the chart of Emmons (1943), using approximate refractive index values, and are probably accurate to within ± 2°. Refractive indices (β) were determined on crushed grains of some of the olivines and clino-pyroxenes from the coarser rocks, nodules and xenocrysts, using immersion media and a refractometer. Longitudinal extinction angles (Z:c) for the clino-pyroxenes were measured on the universal stage on twinned crystals where possible, and supplemented by measurements in slides from sections showing maximum birefringence and flash optical interference figures.

Compositions of the clino-pyroxenes are only broadly determinable from this optical data, particularly the titan-augites, which show wide variations in optical values and compositions (Deer, Howie and Zussman, 1963). However, compositions of some of the clino-pyroxenes in the Corra Linn basalt were determined by micro-probe analysis, through the courtesy of D. H. Green and N. Gray, Australian National University (Table 2).

Plagioclase compositions were estimated from maximum symmetrical extinction angles on albite twins, in conjunction with the determinative procedures of Rittmann and El-Hinnawi (1961). Opaque iron oxides were identified from polished thin sections by reflected light microscope. Potash-bearing feldspars and analcimes were confirmed in a number of cases by etching with HF and staining with sodium cobaltinitrite. Amygdale minerals were determined from optical properties in slides and by X-ray powder photography in a number of cases.

Olivines

The order of crystallisation observed in the Tamar lavas clearly indicates that much of the olivine was present at an early stage, and had suffered partial solution prior to both extrusion and final consolidation, giving corroded phenocrysts. Crystallisation, however, was progressive and separation continued on extrusion, as in almost all cases the phenocryst fraction grades down into groundmass grains. The olivine shows differing degrees of alteration to serpentine, 'bowlingite', carbonates, chlorite and iron ore, and this is marked in the late-stage crystallisations of the coarse lavas.

The olivine ranges from forsterite to hyalosiderite in composition ($2V_z$ 86-105°, $\bumpeq Fo_{94-55}$), with the majority of the crystals showing $2V_z$ between 88-95° ($\bumpeq Fo_{91-76}$). Much of the olivine is zoned, commonly showing more forsteritic cores, and the most fayalitic olivine occurs in the late-stage pegmatites in the coarse lavas ($2V_z$ 95-105°, β 1.730-1.741 ± 0.002, $\bumpeq Fo_{76-55}$). In many rocks some of the phenocrystic olivine shows strain polarisation and translation lamellae, and clearly includes xenocrysts derived from peridotitic xenoliths, described later.

Feldspars

The initial plagioclase crystallised in the Tamar basalts is invariably labradorite, with a composition of about Ab_{3-14}, which on continued crystallisation developed more sodic outer zones, reaching compositions of up to about Ab_{62}. Twinning on the albite, Carlsbad and pericline laws is common. Under conditions of slow cooling that prevailed in the thicker lavas, the plagioclase grew to considerable size, with crystals reaching over a centimetre in length in the coarsest rocks. Investigations of the plagioclases, using the zonal method of Rittmann and El-Hinnawi (1961), indicate that they are high to intermediate-temperature types, including those in the late pegmatitic phases. Some incipient analcimisation of the plagioclase occurs in the coarse analcime bearing basalts.

Late-stage feldspars, with low refractive indices, and commonly negative optical sign and undulose extinction, are developed interstitially in some of the basalts. Their compositions have not been precisely determined, but they include alkali feldspars and sodic plagioclases. Alkali feldspar is a common component in the microlitic mesostasis found in some of the basalts, and also forms overgrowths on plagioclase in the pegmatitic phases of the coarse basalts.

Iron Ore

This is commonly ilmenite or titano-magnetite, generally altered to leucoxene. Its separation covers a wide range during the crystallisation of the lavas. In some cases separation commenced at a very early stage to form the small inclusions within olivine phenocrysts. Much of the iron ore is euhedral to subhedral and crystallised on extrusion, but many of the rocks also show iron ore moulding groundmass minerals and forming skeletal or long lath-like crystals typical of late-stage crystallisation. Finally, in many cases, the mesostases in the rocks are charged with crystallites and globules representing the incipient crystallisation of iron ore just prior to solidification.

Clino-pyroxenes

The clino-pyroxenes in the Tamar lavas include augite, titan-augite and aegirine-augite, and show a wide range in optical properties and textures, reflecting considerable variation in composition and a complex pattern of crystallisation. This is discussed here at some length, but some of the conclusions inferred from the optical data require confirmation by further chemical analyses. Three distinct stages of clino-pyroxene crystallisation can be recognised in the Tamar lavas.

The first stage involved the crystallisation of aluminous augite ($2V_z$ 50-56°, Z:c 47-49°, β 1.698-1.700 ± 0.002) relatively high in sodium and low in calcium content (analyses 1 and 2, Table 2), and is represented as remnant xenocryst cores in the Corra Linn basalt. The chemistry of this augite is consistent with its crystallisation at high pressure, suggesting that the crystals probably separated in the magma at depth and possibly represent the liquidus phase (D. H. Green, pers. comm.). The crystals were presumably carried to the surface out of equilibrium by a rapid ascent of the magma.

The second stage of clino-pyroxene crystallisation is represented by the crystallisation of augite in reaction rims around the augite xenocrysts. This augite ($2V_z$ 50-62°, Z:c 44-52°; analysis 3, Table 2) is lower in alumina and soda and higher in lime compared with the augite cores, and presumably crystallised at lower pressures following reaction and resorption of the cores as the magma rose to higher levels.

The third stage of clino-pyroxene crystallisation is represented by the normal separation of clino-pyroxene about the time of extrusion, and in the Corra Linn basalt this pyroxene mantles the augite of the xenocrysts and their reaction rims. This stage commenced after considerable separation of olivine and usually more or less simultaneously with the crystallisation of plagioclase. In part of the tholeiitic olivine-basalt from 7EX Hill, crystallisation of the clino-pyroxene and feldspar had barely commenced upon chilling into a glassy base containing crystallites and skeletal crystals of these minerals. In the olivine-basalts of the lower Tamar area the crystallisation of the two minerals commenced on extrusion and olivine is the only phenocryst fraction. The porphyritic texture in the basalt at East Arm, correlated with the upper olivine-basalt in the lower Tamar, is interpreted as resulting from prolonged growth of feldspar, and to a lesser extent the pyroxene, below more slowly cooling lava within the neighbourhood of a feeder vent. On the other hand, in the later, widespread, undersaturated olivine-basalts and analcime bearing coarse olivine-basalts, the clino-pyroxene appears to have begun crystallisation by the time of extrusion, giving sporadic, glomeroporphyritic, partly corrosion-riddled phenocrysts, and small, euhedral micro-phenocrysts in the finer grained and chilled contact rocks. Once started, the separation and growth of clino-pyroxene in the Tamar lavas appears to have progressed until solidification was completed.

In the finer grained lavas the bulk of the pyroxene is intergranular, with only limited or incipient intergrowth with the feldspar. In the coarser grained lavas, however, there is also late-stage crystallisation in large subophitic to ophitic plates, apparently formed from growth in slowly cooling parts of thick flows, aided by the presence of volatile-rich residual fluids. In extreme cases, in the pegmatitic phases, the pyroxenes develop complex graphic and dendritic intergrowths. In the nepheline bearing lavas the feldspathoid crystallised at a fairly late stage compared with much of the pyroxene, so that these rocks show groundmass textures ranging from ophitic to poikilitic and grading to hyaloophitic to hyalopilitic.

The normal clino-pyroxenes in the Tamar lavas are augites that are commonly zoned, generally gradationally; normal, reverse, oscillatory, hourglass, complex and colour zoning may be developed. Simple and lamellar twinning on 100 and 010 is often present. The augites show wide variations in optic axial and longitudinal extinction angle values; these are discussed here in relation to the probable compositional trends.

The colourless to pale brown augite in some of the olivine-basalts, and the early colourless augite in the partly corrosion riddled phenocrysts and the inner cores of the titan-augites in the more undersaturated and alkaline lavas, generally shows normal zoning in the range of $2V_z$ 53-66° and Z:c 46-54°. This suggests a diopsidic or salitic augite, probably grading to a composition similar to that in the augite overgrowths around the xenocrysts in the Corra Linn basalt (analysis 4, Table 2).

The incorporation of titanium into the augites to give coloration and pleochroism (X pale pink to mauve, Y pink to reddish mauve, Z pale fawn to yellow brown, $Y > X \bumpeq Z$), no doubt causes complex compositional changes through accompanying balancing substitutions, and gives the wide range observed in optical properties (β 1.705-1.723 ± 0.002). In many of the Tamar rocks the zoned titan-augites, particularly those of late-stage crystallisation, show a general increase in both optic axial and longitudinal extinction angles from core to rim, within the range $2V_z$ 41-77° (core) to 58-84° (rim) and Z:c 33-62° (core) to 38-66° (rim). The higher values commonly, but not always, correlate with a strengthening of colour and pleochroism in the outer zones. These values range notably higher than the normal limits of $2V_z$ and Z:c for augites (including titan-augites), except for sodian augites (Deer, Howie and Zussman, 1963). This, considered in conjunction with marginal gradation and alteration of a number of these titan-augites into greenish aegirine-augite (Z:a 46-18°; inner zone to rim), suggests that the high values may be due to the incorporation of significant amounts of sodium, possibly as a solid solution of titan-augite and soda-augite. Such intermediate clino-pyroxenes have been described by Yagi (1953) from alkaline rocks in the Sakhalin area, and it is interesting to note that the host dolerites show a similar chemistry to the coarse olivine-basalts of the Tamar suite.

In contrast, some of the titan-augites of the Tamar lavas show a decrease of optic axial angle and an increase of longitudinal extinction angle from core to rim, within the range $2V_z$ 52-66° (core) to 41-53° (rim) and Z:c 34-49° (core) to 38-54° (rim). This tends to occur in the finer grained lavas and is more typical of the normal trend in zoned augite (Wilkinson, 1956b; Deer, Howie and Zussman, 1963); sodium presumably has not entered into these augites to any great degree.

An interesting comparison can be made with the trends in optical behaviour of titan-augites of the Tamar lavas and the similar Auckland basalts of New Zealand (Searle, 1961). The typical titan-augite of the Auckland basalts generally forms small crystals in fine grained lavas, with $2V_z$ 56-72° and Z:c 41-52°, and almost universally the 2V values decrease and Z:c values increase from the inner to outer zones. On the other hand, in rare coarse phases with strongly coloured, zoned titan-augite $2V_z$ and Z:c both increase from paler inner zones to darker outer zones, e.g., in the Domain basanite with $2V_z$ 42-48° (inner zone) to 63-64° (outer zone) and Z:c 47-52° (inner zone) to 54-61° (outer zone). Thus, there is a parallelism in the titan-augite trends of the two suites, but in the Tamar rocks the trend shown by the late-stage titan-augite is much more prominent, probably largely as a result of slower cooling and crystallisation in thicker lavas.

A further trend is also noted in the Tamar rocks in cases where titanium depletion has reversed the typical late-stage trend. These titan-augites have paler coloured outer rims that show a decrease in both $2V_z$ and Z:c within the range $2V_z$ 59-66° (inner zone) to 41-53° (outer zone) and Z:c 47-49° (inner zone) to 41-42° (outer zone). These values suggest that with the titanium depletion sodium may also be lost from the augite structure and accommodated in the residual mesostasis of the rock.

Finally, clino-pyroxenes have crystallised in a number of the Tamar lavas through reaction with incorporated sedimentary xenoliths. This clino-pyroxene occurs within the fused xenoliths and/or around them in reaction rims; sporadic clino-pyroxene aggregates in the rocks probably represent the extreme case of this replacement. The clino-pyroxene is colourless to pale brown or mauve and is commonly prismatic. Measurements on zoned crystals gave $2V_z$ 67° (core) to 58° (rim) and Z:c 43° (core) to 53° (rim). Similar clino-pyroxene replacements are described in xenoliths in the Auckland basalts by Searle (1962) and his detailed remarks on their formation are probably equally applicable to those of the Tamar rocks.

Feldspathoids and Accessory Minerals

Nepheline is represented as a major constituent in the olivine-nephelinites and the nepheline-basanite of the Tamar suite. It generally forms poikilitic areas in a glassy groundmass, but becomes more coarsely crystalline in some phases and forms large zoned crystals up to over 5 mm in length in the nephelinite pegmatite at Spring Bay. No detailed analytical or optical work was done on the nepheline. Analcime occurs in the coarse olivine-basalts as interstitial fillings, and staining tests indicate that some of the analcime is potash-bearing. Apatite is invariably present, ranging from small needles in the mesostasis to coarse elongated prisms. Small prisms and needles of aegirine-augite and small flakes of biotite are common minor accessories in the rocks containing an alkaline mesostasis.

Mesostases

The majority of the Tamar lavas contain glassy or microlitic mesostases that in some cases form a considerable proportion of the rock. Glassy mesostases are developed in the finer grained rocks and microlitic mesostases are best developed in the coarse olivine-basalts. The tholeiitic olivine-basalt from 7EX Hill contains an abundant black, opaque, glassy mesostasis typical of such basalts in Tasmania, but in the alkaline lavas the glassy mesostasis is commonly a clear to cloudy glass containing crystallites, and in some cases passes into a brown glass darkened with incipient crystallisation of iron ore. Four gradational mesostases can be recognised in the coarse basalts. Mesostasis type 1 consists largely of intersertal sodic plagioclase, associated with small prisms and crystallites of titan-augite, commonly altered to aegirine-augite, grains and globules of iron ore, some zeolite and clear glass. Mesostasis type 2 is similar, but zeolite predominates and consists mainly of analcime and fibrous radiating species. Mesostasis type 3 consists of numerous small laths and curved to spherulitic microlites of alkali feldspar, associated with prisms of apatite, small grains and crystallites of iron ore and flakes of biotite, in a zeolitic analcime-rich base containing indeterminate chloritic or serpentinitic material. Mesostasis type 4 resembles type 3, but lacks the indeterminate greenish material. Mesostasis types 3 and 4 are typically developed in the pegmatitic phases, in some cases forming over half the rock. A further mesostasis in the lower olivine-basalt in the lower Tamar consists largely of carbonates (including siderite) and chloritic, nontronitic or serpentinitic clays, and rarely a zeolite resembling chabazite.

Amygdale, Joint and Vein Minerals

Opal, chalcedony, carbonates and clays are common secondary minerals in the tholeiitic olivine-basalt of 7EX Hill and the lower olivine-basalt in the lower Tamar. Zeolites are common in amygdales and veinlets in the alkaline lavas and include natrolite, scolecite, stilbite, thomsonite, phillipsite and chabazite. Other accompanying minerals that may be present are apophyllite, gyrolite, diaspore or gibbsite (?), carbonates and clays. Pyrite coats joint planes in the lower olivine-basalt in the lower Tamar.

Xenoliths

A number of the Tamar lavas carry accidental xenoliths of the country rocks. Small fused and partially replaced pieces of Tertiary sediments are relatively common. Xenoliths of Jurassic dolerite, in which the mesostasis has been partly fused and recrystallised, were noted in the Corra Linn basalt and in the olivine-nephelinite east of St Leonards.

Small peridotite xenoliths occur in the olivine-nephelinites at Spring Bay and east of St Leonards, in the nepheline-basanite at Deviot, in the coarse olivine-basalt on the East Arm foreshore, and in the pyroxene-olivine-basalt at Corra Linn. They are composed mostly of olivine and some clinopyroxene. The olivine commonly shows strain polarisation and translation lamellae, and gave $2V_z$ 86-94° and β 1.667-1.678 ± 0.002, indicating compositions within the range Fo_{94-76}, and mostly within Fo_{92-86}. The clino-pyroxene ($2V_z$ 53-67°, Z:c 46-50°, β 1.688-1.692 ± 0.002) is a colourless, aluminous augite that approaches an endiopsidic composition, judging from the analysis from basalt at Blessington (analysis 6, Table 2). The peridotites also contain minor enstatite, calcic plagioclase ($\bumpeq Ab_{10-37}$) and green, brown or grey spinels, including ferroan varieties (analysis 5, Table 2).

Similar peridotite nodules are known elsewhere in Tasmania (Sutherland, 1969b), on the Australian mainland (Joplin, 1964) and in New Zealand (Searle, 1961; Black and Brothers, 1965); their distribution is world-wide in basaltic rocks (Green and Ringwood, 1967). Their origin has been disputed; some consider them disrupted segregations and accumulations of crystallates within magma chambers (Searle, 1960-1961; Brothers, 1960; Wager, 1962; etc.), others consider that they are probably derived from the mantle (Turner and Verhoogen, 1960; Wilshire and Binns, 1961, etc.). This question has been reviewed by Black and Brothers (1965) following detailed textural studies on nodules from Tokatoka, New Zealand, and more recently by Green and Ringwood (1967). The latter consider lherzolitic types as remnants derived from the mantle; other types, such as the olivine-augite types in the Tamar lavas, may be genetically distinct.

DIFFERENTIATION IN THE TAMAR LAVAS

Differentiation trends

These can be distinguished in the Tamar suite, both between separate lavas and within individual lavas, by reference to the variation diagram for plots of their solidification index (Kuno, 1959) against SiO_2, Na_2O and K_2O (Figure 4).

The lower olivine-basalt in the lower Tamar (analysis 1, Table 1) plots as the least 'differentiated' of the Tamar lavas on this diagram, suggesting that it may represent a composition close to its parent magma. The Corra Linn basalt with its complement of augite xenocrysts from depth (analysis 9, Table 1) also plots as a little 'differentiated' lava. Another plot with a solidification index over 40 is the picritic phase of the coarse olivine-basalt of the middle Tamar, but in this case differentiation within the basalt itself has spread the apparent values (analyses 4-6 and 13, Table 1), and the average of these suggests slightly 'differentiated' lava.

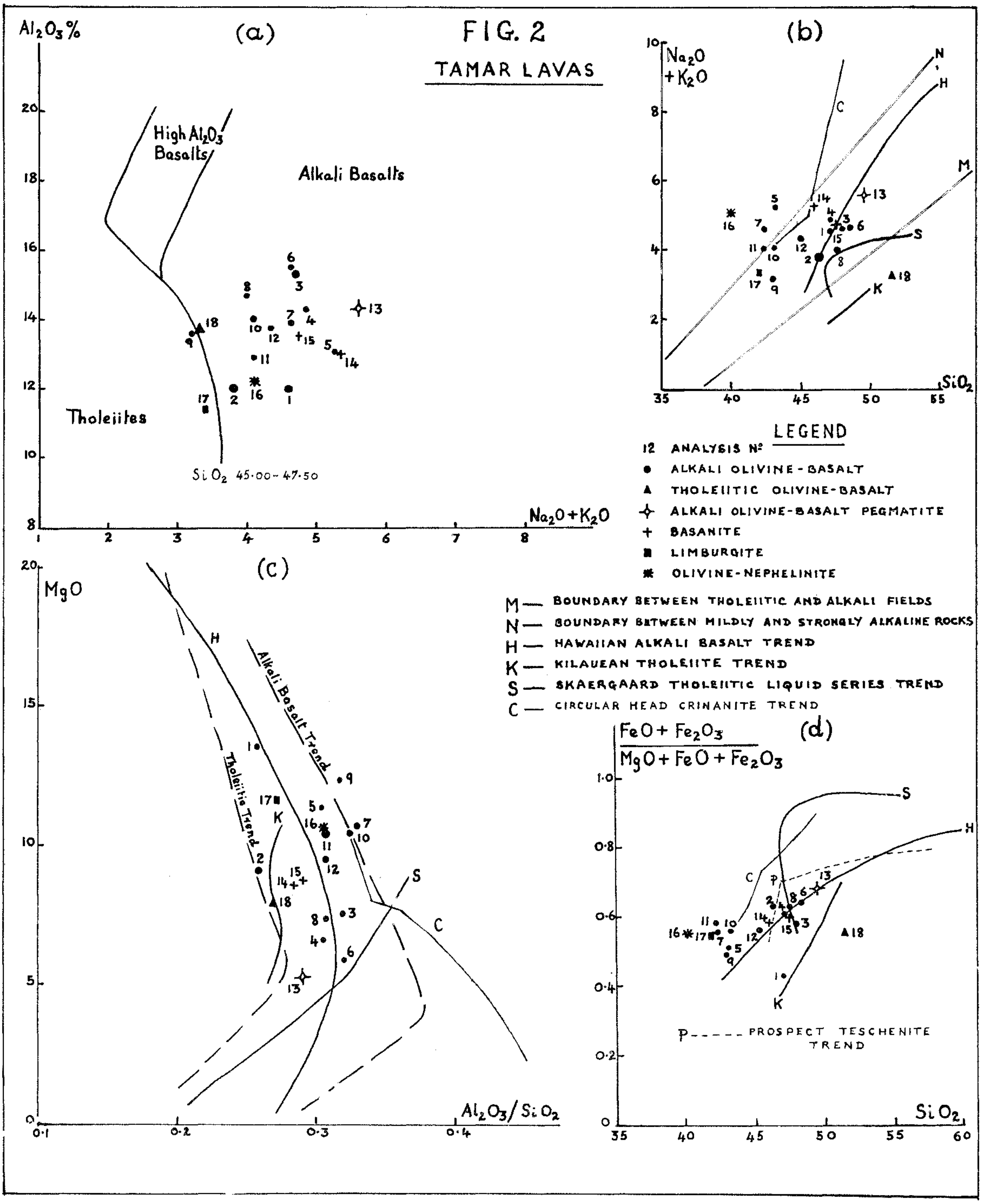

FIGURE 2—Chemical variation diagrams of the Tamar lavas: (*a*) Al_2O_3 v $Na_2O + K_2O$ with basal field boundaries from Kuno (1960, $SiO_2$45.00-47.50); (*b*) $Na_2O + K_2O$ v SiO_2, with tholeiite-alkali basalt boundary (M) from MacDonald and Katsura (1964), and boundary of mildly and strongly alkaline rocks (N) from Saggerson and Williams (1964); (*c*) MgO v Al_2O_3/SiO_2 with alkali basalt and tholeiite trends after Murata (1960); (*d*) FeO + Fe_2O_3/MgO + FeO + Fe_2O_3 v SiO_2; S (trend of Skaergaard liquid series, Wager 1960); K (Kilauean tholeiitic trend, Tilley 1960, Muir and Tilley 1963); H (Hawaiian alkali basalt trend, MacDonald 1949); C (Circular Head crinanite trend, from analyses of Edwards 1941); P (Prospect teschenite trend, Wilshire 1967).

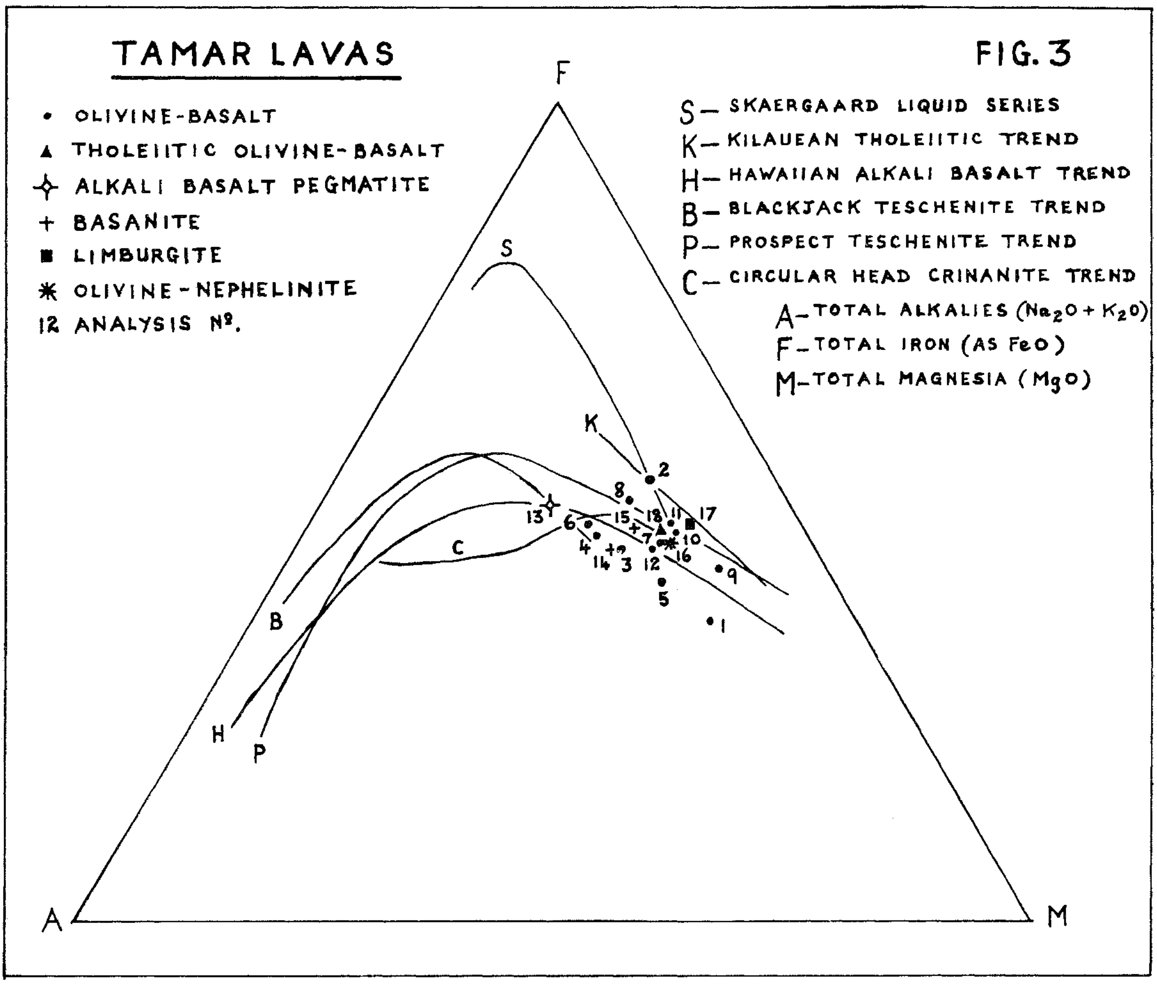

FIGURE 3—FMA ternary chemical variation diagram of the Tamar lavas; F, total iron as FeO; M, total magnesia as MgO; A, total alkalies as $Na_2O + K_2O$; S (trend of Skaergaard liquid series, Wager 1960); K (Killauean tholeiitic trend, Tilley 1960, Muir and Tilley 1963); H (Hawaiian alkali basalt trend, MacDonald 1949); B (Black Jack teschenite trend, Wilkinson 1958); P (Prospect teschenite trend, Wilshire 1967); C (Circular Head crinanite trend, from analyses of Edwards 1941).

Most of the Tamar lavas, if internal differentiation is discounted, fall in the field of slightly 'differentiated' rocks with solidification indices between 30 and 40. The nepheline-basanite (analysis 14) appears to be a slightly 'differentiated' variant of the undersaturated titan-augite olivine-basalts of the Tamar (analyses 7, 10 and 11, Table 1). The olivine-nephelinite (analysis 16, Table 1) with its solidification index of over 35 appears relatively little modified by differentiation, and the limburgite (analysis 17, Table 1), with its solidification index greater than the majority of the lavas, suggests an early derivative.

Variations in modal mineralogy, texture, chemical composition and solidification index in the coarse basalts of the Tamar suggest differentiation within the thicker parts of these flows (Plates 6, 7 and 8; analyses 4, 5, 6, 8 and 13, Table 1; Figure 4). This is most marked in the middle Tamar area and basalts were sampled here from four levels at East Arm for chemical analysis: from picritic basalt in the lower levels of a basalt fill at river level (analysis 5); from 150 feet above river level in the upper part of the fill, from olivine-poor, mesostasis-rich basalt (analysis 6); from basalt capping the hill at about 250 feet, adjacent to the fill (analysis 4), presumably representing less differentiated basalt; and from pegmatite at 350 feet (analysis 13), presumably representing a late-stage differentiate of the basalt capping. The analyses reflect the general modal compositions of the rocks; the picritic phase shows relative enrichment in magnesia and ferrous iron and impoverishment in silica, alumina and ferric iron, compared with the basalt of the flow capping, and the mesostasis-rich and pegmatitic phases show relative enrichment in silica, alumina and ferric iron, and impoverishment in magnesia and ferrous iron. This differentiation trend is seen in the chemical variation diagrams (Figures 2, 3 and 4), and the solidification indices of the rocks spread from over 45 for the picritic phase to less than 25 for the pegmatitic phase, thus passing into the field of moderately strongly differentiated rocks. Coarse olivine-basalt from the upper part of the flow, south of Atkinsons Creek in the upper Tamar, also shows relatively low magnesia and high alumina and silica, suggesting some differentiation (analysis 8).

Differentiation and Behaviour of Titanium in the Clino-pyroxenes

Differentiation within the Tamar lavas has produced two trends of crystallisation of the pyroxenes in regard to the behaviour of titanium, often discriminated in alkali rocks (Yagi and Onamu, 1967); i.e., an initial trend of titanium enrichment in the earlier stages of fractionation, and a reverse trend of titanium depletion in the later stages of differentiation. Evidence of titanium enrichment in pyroxenes during early stages of fractionation is found in the following cases:—

(1) in the upper basalt in the lower Tamar and in the limburgite in the south Tamar, in which later stage pyroxenes crystallising in the mesostasis take on deepening coloration compared with the near colourless earlier groundmass pyroxene;

(2) in the undersaturated olivine-basalts and coarse olivine-basalts in which early pyroxenes with corrosion riddling are essentially colourless compared with coloured pyroxenes in the bulk of the rock;

(3) in the undersaturated olivine-basalts and coarse basalts, in which there is deepening of colours towards the outer zones of the pyroxene crystals, becoming particularly marked in the late-stage ophitic plates or in the presence of an abundant microlitic mesostasis;

(4) in the pyroxene-olivine-basalt from Corra Linn, in which the pyroxene overgrowths around the augite xenocrysts show a progressive change outwards from colourless to coloured augite.

Evidence of titanium depletion in pyroxenes during the later stages of fractionation in the Tamar rocks is found—

(1) in the late-stage pegmatitic veins and segregations in the coarse olivine-basalts and olivine-nephelinite, in which some of the titan-augites show paler coloured outer zones;

(2) in the coarse basalts in which titan-augite in contact with, or within the late-stage mesostasis is altered to greenish aegirine-augite, as these soda pyroxenes are generally poor in titanium relative to titan-augite (see Yagi and Onamu, 1967; Deer, Howie and Zussman, 1963: Tables 12 and 20).

Differentiation within Lavas

The available evidence suggests that the coarse basalts of the Tamar probably represent flows several hundred feet in thickness. Such thicknesses of lava would cool relatively slowly and seem adequate for differentiation to take place, based on known thicknesses of differentiated sills (200-700 feet thick) of similar rock composition elsewhere in Australia (Joplin, 1964). Differentiated sills such as the Prospect and Black Jack teschenite bodies in New South Wales (Wilshire, 1967; Wilkinson, 1958; Joplin, 1964) and the differentiated 'crinanite' in necks at Circular Head and Table Cape (Edwards, 1941; Gill and Banks, 1956; Gee, 1966), resemble the coarse basalts of the Tamar in many petrological features, although they show differences in details of differentiation.

The Circular Head and Prospect rocks crystallised from a parent magma of similar composition to that of the coarse basalt of the Tamar, but the Black Jack body crystallised from a slightly more alkaline magma, and all the differentiates are nepheline-normative, unlike some of the Prospect and Tamar rocks. The differentiation process in the sills and necks appears more pronounced than in the Tamar lavas, and the highly alkaline differentiates of these bodies, such as analcime-syenite and theralite were not noted in the Tamar rocks. Differences in compositional trends of the mineralogical phases separating during crystallisation can be noted, as on comparing the olivines and clino-pyroxenes of the Black Jack and Tamar rocks. The late olivine in the Black Jack sill (Wilkinson, 1956a) shows greater iron enrichment than that in the late pegmatites of the coarse basalts of the Tamar, and this is presumed to reflect more lengthy cooling in a sill compared with a lava of comparable thickness. In the clino-pyroxenes of the Black Jack sill, Wilkinson (1957) notes an increase in reverse zoning with $2V$ margin $>$ $2V$ core as in the later titan-augite in the Tamar rocks. However, here, the increase appears to be due to the introduction of magnesium, and the titan-augites show decreased titanium contents, no significant increase in sodium content, and in contrast lack the extreme high values of $2V_z$ and Z:c shown by the Tamar titan-augites.

Comparison of the differentiation trends of the Black Jack, Prospect and Circular Head bodies plotted in the variation diagrams in Figures 2, 3 and 4, with that of the coarse basalt of the middle Tamar (analyses 4-6 and 13) reveals some interesting differences. The Tamar trend differs markedly from that of the Circular Head 'crinanite' trend, and although it again shows some differences, lies more closely to the femic extension of the Black Jack and Prospect trends. This suggests that the differentiation processes operating in thick flows of alkaline magma approach those shown by sills rather than necks.

Coarse olivine-basalt closely matching the Tamar basalts is also found in Tasmania at Mt Cameron West, apparently forming a single flow over 500 feet thick (Gill and Banks, 1956; Sutherland and Corbett, 1967). However, the rock at Mt Cameron West is not much differentiated and no marked pegmatitic or picritic phases were noted. This may have resulted from the lava here filling a narrower valley than in the Tamar and probably cooling more quickly relative to the process of differentiation. Thus, not only a sufficient depth, but also a sufficient width of lava, appears to be required for noticeable differentiation to take place in such flows.

The pegmatites of the Tamar basalts represent the extreme phase of the differentiation, with enrichment of silica, titania, soda and potash, at the expense of magnesia and lime. They occur mostly in the lower levels of the flows, showing that the parent residual fluids accumulated deep within the flows without wholesale migration into the upper levels; rocks with coarser ophitic textures and deeper coloured titan-augite are also found in the lower half of the Mt Cameron West flow. This behaviour contrasts with that normally found in differentiated sills, where the coarsest rocks and pegmatites tend to form in the upper levels, e.g., Black Jack, Prospect and Tasmanian Jurassic dolerite sills (Wilkinson, 1958; Wilshire, 1967; Joplin, 1964). This, no doubt, results from relatively more rapid chilling and crystallisation in the upper levels of flows, arising from a more unequal temperature gradient from top to bottom, compared with sills.

Fractionation trends of basalt magmas in lava flows are discussed by Kuno (1965) but his examples are drawn from tholeiites, high-alumina basalts and basaltic andesites rather than alkali basalts. Kuno considers that different trends in total iron and silica contents during differentiation arise largely from differences in oxygen partial pressure, probably due to differences in the initial water contents of the magma. The coarse basalt in the middle Tamar shows a typical alkali basalt trend of increasing silica and nearly constant total iron, which according to Kuno would indicate a high oxygen pressure and hence probably a high initial water content. The presence of abundant pegmatites and mesostasis-rich phases in the basalt, carrying hydrous minerals such as analcime, other zeolites, biotite and chlorite fully supports this.

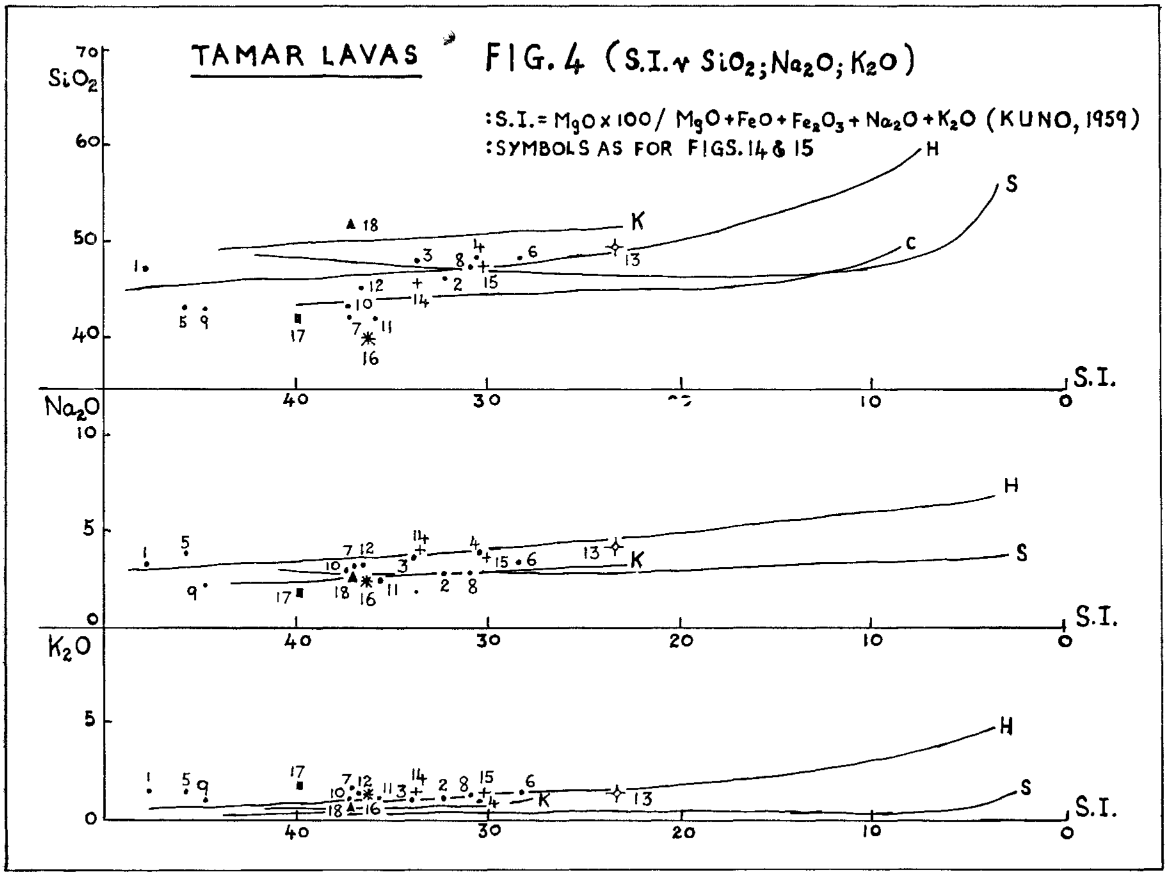

FIGURE 4—Solidification index chemical variation diagrams of the Tamar lavas: S.I. (solidification index, Kuno 1959) v SiO_2, Na_2O, K_2O; S (trend of Skaergaard liquid series, Wager 1960); K (Kilauean tholeiitic trend, Tilley 1960, Muir and Tilley 1963); H (Hawaiian alkali basalt trend, MacDonald 1949); C (Circular Head crinanite trend, from analyses of Edwards 1941) N.B.—The reference to Figs. 14 and 15 in Fig. 4 should read as Figs. 2 and 3.

PETROCHEMICAL AFFINITIES OF THE TAMAR LAVAS

The Tertiary volcanic rocks of the Tamar Trough range from undersaturated lavas such as olivine-nephelinite, nepheline-basanite and limburgite through undersaturated and near-saturated olivine-basalts to saturated olivine-basalt. The bulk of the lavas are undersaturated to near-saturated olivine-basalts, with the other rocks only forming small restricted flows. In general, the Tamar suite can be regarded as predominantly an alkaline association, with minor tholeiitic lava, as discussed later. In this study the petrochemical affinities of the Tamar lavas are examined in relation to similar Cainozoic volcanic associations in the Australasian region and then compared with a few of the well-known petrographic suites elsewhere in the world.

Australasian Affinities

Alkaline volcanic suites similar to the Tamar lavas are found elsewhere in Tasmania (Edwards, 1950; Spry, 1962; Sutherland, 1969a, 1969b); in eastern Australia, best typified by the Older Volcanic series of Victoria (Edwards, 1939, 1950); and in New Zealand, best typified by the Auckland Basalts (Searle, 1961). The available petrochemical data on the Tasmanian Cainozoic volcanic province (including that of the Tamar suite) is discussed by Sutherland (1969b) and a further analysis is not attempted here. Detailed petrochemical data are scanty for the Older Volcanic series of Victoria, but the average calculated basalt (Edwards, 1939) compares closely with that of the Tamar suite (analysis 12, Table 1). Detailed petrochemical data has been presented for the Auckland Basalts (Searle, 1961), enabling a close comparison with the Tamar suite.

The Tamar alkali basalts (analyses 1 to 11, Table 1) chemically resemble the Auckland basalts in degree of silica undersaturation, in relatively high alkali contents, and in alumina contents mostly in excess of magnesia and present in approximately sub-equal amounts with lime and ferrous oxide. The average calculated composition of the Tamar basalts (analysis 12, Table 1) is very close to that of the average Auckland basalt and indicates a similar parent magma, chemically intermediate between the ' normal alkaline basalt ' and the ' olivine-rich alkaline basalt ' of Nockolds (1954). The Tamar basalts, however, tend to be somewhat richer in iron oxide at the expense of magnesia, and this is probably reflected in the relatively more common occurrence of picrite basalts amongst the Auckland lavas.

Norms calculated for the Tamar basalts (Table 1) resemble those of the Auckland basalts in that some of the rocks show noticeable amounts of normative nepheline, which finds little or no modal expression. In the Auckland rocks the excess soda is apparently incorporated into the residual groundmass feldspar and mesostasis. The Tamar basalts show a similar behaviour, although in the coarser basalts the excess soda appears as analcime. Further, the presence of titaniferous augites in the rocks will increase the available silica by substitution (probably Ti for Mg. accompanied by Al for Si; see Yagi and Onamu, 1967), and in reality diminish the apparent values of normative nepheline. Some of the Tamar basalts also contain aegirine-augite and sodian titan-augites (judging from their optical properties as previously discussed), and this would also use some of the available soda.

Some of the Tamar basalts approach basanites in regard to their chemistry and calculated normative nepheline, but mineralogically they are olivine-basalts grading to analcime bearing olivine-basalts. Rocks termed basanites in the Tamar suite and elsewhere in Tasmania, and on mainland Australia, generally show slightly greater alkali contents (analysis 14, Table 1; Spry, 1962, analyses 108-109; Joplin, 1963, Tables N and O), as does the average teschenite (and corresponding lavas) of Nockolds (1954). Of particular interest in this respect is the nepheline-basanite at Deviot, with about 8% modal nepheline, which grades into an analcime bearing coarse olivine-basalt, with only a slight decrease in alkalies and a slight increase in silica (analysis 15, Table 1). This indicates strong sensitivity between the chemistry and mineralogy in these rocks.

The general lack of modal nepheline in basalts in the presence of high normative nepheline is typical of the rocks belonging to the alkali-rich, sub-aluminous associations of the Pacific Basin (Barth, 1931). The alkali and calcic contents of the Tamar rocks, with the field of the Auckland Basalts for comparison, are plotted on a ternary diagram (Figure 1) similar to that used by Searle (1960), after Green and Poldervaart (1958). The diagram plots the relative number of ions of K-Na-Ca (data from Table 1) and illustrates the close affinities of the Tamar and Auckland suites, and the distribution relative to the trend lines recognised by Green and Poldervaart. The Tamar suite, as does the Auckland suite, lies along trend B, and thus, although chemically comparable with the lavas from the sub-aluminous alkaline associations of the Pacific Basin, is possibly derived by fractionation along a trend more characteristic of a continental environment (Searle, 1960).

Relationships to Some Overseas Petrographic Provinces

The petrochemistry of the Tamar suite (analyses 1-18, Table 1) is plotted on a number of variation diagrams (Figures 2, 3, and 4) and compared with trend lines of the well known Skaergaard liquid series (Wager, 1960), the Kilauean tholeiitic rocks (Tilley, 1960; Muir and Tilley, 1963) and the Hawaiian alkali basalts (MacDonald, 1949).

In the diagram for alumina against total alkalies (Figure 2a), with basalt field boundaries from Kuno (1960) for SiO_2 45.00-47.50, the Tamar suite plots from the tholeiitic field into the alkali basalt field, with no plots in the high-alumina basalt field. The tholeiitic olivine-basalt from 7EX Hill (analysis 18) occupies a position between the two fields, but would fall in the tholeiite field using the appropriate SiO_2 50.01-52.50 boundary of Kuno. In the FMA diagram (Figure 3) it falls between the Kilauean tholeiite and Hawaiian alkali basalt trends, near the Skaergaard trend. However, in the diagram for silica against total alkalies (Figure

2b) it clearly falls within the tholeiite field of MacDonald and Katsura (1964), and in the diagrams for SiO_2 against $FeO + Fe_2O_3/MgO + FeO + Fe_2O_3$ (Figure 2d), for MgO against Al_2O_3/SiO_2 (Figure 2c) after Murata (1960), and for Kuno's (1959) solidification index against SiO_2, Na_2O and K_2O (Figure 4) it is associated with the Kilauean tholeiitic trend.

The limburgite from 'Duneiden Farm' (analysis 17) plots with the alkali basalts in a number of the variation diagrams, but in the FMA diagram (Figure 3) it plots on the Kilauean tholeiitic trend. In the diagram for alumina against total alkalies (Figure 2a) it again plots in the tholeiite field, although allowance for its undersaturated composition to the SiO_2 45.00-47.50 boundary of Kuno (1960) must be made. This suggests that the limburgite may be derived from a tholeiitic olivine-basalt parent, a possibility strengthened by its close field association with the 7EX Hill tholeiitic olivine-basalt.

The alkali olivine-basalts of the Tamar, as plotting in the diagram for silica against total alkalies (Figure 2b), form a suite of mildly alkaline basalts overlapping into the field of strongly alkaline basalts, relative to the boundary after Saggerson and Williams (1964). In the variation diagrams they plot near the Hawaiian alkali basalt trend, with two main exceptions. In the diagram for alumina against total alkalies (Figure 2a) the pyroxene-olivine-basalt from Corra Linn (analysis 9) plots in the tholeiite field, but this is due to the numerous xenocrysts of aluminous augite in the rock, reducing the relative alumina and alkali content, and to its undersaturated composition in respect to the SiO_2 45.00-47.50 boundary of Kuno (1960). Again, the upper olivine-basalt from the lower Tamar area (analysis 2), although plotting as an alkali basalt in Figures 2b, 2d and 4, plots on the Kilauean tholeiite trends in Figures 2c and 3, due to its relatively high iron content.

The alkaline rocks represented by the more differentiated phases and the pegmatite of the coarse olivine-basalts (analyses 4, 6, 8 and 13), and the nepheline-basanite from Deviot (analyses 14 and 15), tend to plot as an extension of the olivine-basalts along the trend of the Hawaiian alkali basalts. Overall, the variation diagrams indicate that the Tamar alkali basalt trend approaches that of the Hawaiian basalts, with the Tamar rocks tending to be enriched in alkalies and impoverished in magnesia in respect to silica (Figures 2b, 2d). Thus, in the FMA diagram (Figure 3), the differentiated alkaline-rich, analcime bearing, coarse basalt from the middle Tamar (analyses 4, 5, 6 and 13) plots towards the extension of the Black Jack teschenite trend of Wilkinson (1958). The olivine-nephelinite from Spring Bay (analysis 16) plots away from the Tamar and Hawaiian alkali basalt trends in some of the variation diagrams (Figures 2b, 2d and 4), a point discussed later.

THE ERUPTIVE AND MAGMATIC HISTORY OF THE TAMAR LAVAS

The Eruptive Succession

The Tamar extrusions have been dated to a limited extent from the field stratigraphy, but precise datings will require detailed radiometric and palaeomagnetic studies.

From presently available evidence the eruptive sequence tentatively suggested for the Tamar volcanism is: initial eruptions of near-saturated alkali olivine-basalts in the lower and south Tamar areas during the Lower Tertiary, probably post-Middle Eocene and pre-Upper Oligocene; then extrusion of olivine-nephelinite in the middle Tamar area in the Lower to Middle Tertiary, probably in the Oligocene; and finally effusions of undersaturated alkali olivine-basalts and nepheline-basanite, followed by thick coarse alkali olivine-basalts in the middle, upper and south Tamar areas in Middle or Upper Tertiary time, probably post-Upper Oligocene and pre-Middle Pliocene. The positions in this sequence of the small extrusions of olivine-nephelinite, tholeiitic olivine-basalt and limburgite in the south Tamar are unknown.

Genesis of the Tamar Lavas

The Tamar lavas form essentially an alkaline suite, apparently derived from alkali basalt parent magmas. Recent work on genesis of basalts (Green and Ringwood, 1967) suggest that such parent magmas may be generated by relatively restricted degrees of direct partial mantle melting, with segregation of the alkali basalt magmas at depths of 35-70 Kms.

The initial magma appears to have ascended in a fairly undifferentiated state to form the lower olivine-basalt in the lower Tamar (solidification index > 45, Figure 4), but then underwent some differentiation prior to further eruption to form the upper olivine-basalt (solidification indices $< 35 > 30$).

The next phase appears as minor extrusion of olivine-nephelinite in the middle Tamar, and possibly in the south Tamar. This may represent more extreme differentiation of the initial alkali-basalt magma, but its relatively high solidification index, and its tendency to plot away from the alkali basalt trend in variation diagrams, infers a somewhat different origin. Recent work by Bultitude and Green (1968) suggests that such rocks may form during waning in volcanism under a low degree of melting, giving more hydrous conditions that allow fractionation of alkali basalt magma towards such undersaturated compositions at depths of 60-100 Kms.

This was followed by the eruption of undersaturated olivine-basalts in the upper and south Tamar, presumably following renewed, more widespread generation and segregation of alkali basalt magma at depths of 35-70 Kms. These basalts approach basanites in composition and show solidification indices between 45-35. The augite xenocrysts in the Corra Linn basalt suggests that magma may have formed by fractional crystallisation of this augite from a more primitive parent. Crystallisation of augite of such composition points to a parent magma richer in silica, lime and magnesia and somewhat poorer in iron, alumina and alkalies, but rocks of such composition are unknown in the Tamar suite. Alternatively, however, if fractionation proceeded by crystallisation of olivine and/or spinel, as well as augite, then this provides for relatively constant compositions in regard to lime and would give a parent magma approaching the composition of the lower olivine-basalt in the lower Tamar, but a little poorer in alkalies. Whether the olivine-augite nodules found in the rocks represent products of such fractionation is uncertain without more detailed work.

The final phase of the volcanism includes the extrusion of the coarse olivine-basalts in the middle, upper and south Tamar areas and possibly the nepheline-basanite in the middle Tamar. These lavas tend to show slight enrichment in silica, alkalies and alumina compared with the preceding undersaturated olivine-basalts. This may reflect some differentiation within the undersaturated magma at relatively higher levels and lower pressures, as low pressure differentiation along similar trends continued within the thick lavas after extrusion.

The tholeiitic olivine-basalt, and possibly the alkali-poor limburgite, in the south Tamar area form the western outskirts of a tholeiitic olivine-basalt association to the south-east and east, overlapping into the alkaline suite of the Tamar Trough. Following the studies of Green and Ringwood (1967), the parent tholeiitic magmas for this association may have formed as the result of relatively higher degrees of partial mantle melting, with segregation of magma at depths of 35-70 Kms. In the broad context, the Tamar Trough falls within an alkaline volcanic association extending to the west as far as the Devonport-Deloraine area (interpreted as possibly representing an area of lesser mantle melting), but its south-eastern end passes transitionally into a dominantly tholeiitic association extending to the east as far as the Camden Plains-Avoca area (interpreted as possibly representing an area of greater mantle melting). The overall aspects of the Cainozoic volcanism of the Tasmanian province, including that of the Tamar Trough, are reviewed elsewhere (Sutherland, 1969b).

TABLE 1

Chemical Analyses and Molecular Norms—Tamar Tertiary Lavas

Analysis	1	2	3	4	5	6	7	8	9	10	11	12	13	14	15	16	17	18
SiO_2	47.04	46.3	47.93	47.21	43.12	48.40	42.3	47.5	43.0	43.2	42.2	45.18	49.53	45.95	47.48	40.0	42.0	51.52
Al_2O_3 ..	12.05	12.0	15.28	14.26	13.07	15.49	13.9	14.7	13.6	14.0	12.9	13.75	14.34	13.05	13.49	12.2	11.4	13.76
Fe_2O_3.. ..	0.31	3.7	1.43	1.01	0.93	3.61	4.3	2.8	4.1	4.4	4.7	2.84	2.84	1.53	2.15	3.9	4.0	1.43
FeO	9.98	11.6	8.78	9.33	10.83	6.67	9.2	9.8	8.0	9.2	10.0	9.40	8.76	10.29	10.45	10.7	10.4	8.78
MnO	0.24	0.20	0.19	0.15	0.13	0.21	0.1	0.20	0.17	0.1	0.22	0.17	0.18	0.24	0.19	0.24	0.2	0.18
TiO_2	1.82	2.2	2.00	2.15	2.53	2.25	2.3	1.6	2.3	2.3	2.2	2.15	3.21	2.42	2.37	2.8	2.5	1.78
P_2O_5	0.53	0.59	0.83	0.42	0.44	0.44	1.53	0.51	0.62	0.79	0.86	0.69	0.62	0.98	0.42	1.2	0.83	0.18
CaO	8.34	8.2	10.00	9.26	9.67	9.69	10.9	9.5	11.2	11.1	9.3	9.74	8.41	10.02	8.07	9.4	11.3	8.46
MgO	13.59	9.1	7.60	6.64	11.46	5.89	10.7	7.4	12.4	10.5	10.5	9.62	5.27	8.58	8.76	11.2	11.7	7.95
Na_2O	3.20	2.8	3.54	3.77	3.83	3.37	3.06	2.7	2.2	3.03	2.5	3.09	4.05	4.11	3.61	3.6	1.8	2.65
K_2O	1.41	1.0	1.15	1.09	1.44	1.27	1.56	1.3	1.0	1.07	1.6	1.26	1.56	1.18	1.11	1.5	1.6	0.64
Ignition Loss	2.13	1.3	1.45	3.52	1.57	1.59	1.05	1.5	0.94	0.80	1.7	1.59	1.45	2.05	2.80	2.0	1.12	1.69
H_2O^- ..	0.65	0.71	0.64	0.40	0.16	0.34	0.10	0.67	0.84	0.16	1.1	0.52	0.64	0.48	0.57	0.89	0.40	0.15
Total ..	101.29	99.70	100.82	99.21	99.42	99.22	100.90	100.18	100.37	100.65	99.78	100.00	100.86	100.88	101.47	99.63	99.25	99.17

TABLE 1—*Chemical Analysis and Molecular Norms—Tamar Tertiary Lavas—contd.*

C.I.P.W. Norm	1	2	3	4	5	6	7	8	9	10	11	12	13	14	15	16	17	18
Q	0.00	0.00	0.00	0.00	0.00	0.00	0.00	0.00	0.00	0.00	0.00	0.00	0.00	0.00	0.00	0.00	0.00	2.25
Or	8.33	5.91	6.80	6.44	8.51	7.51	9.22	7.68	5.91	6.32	9.46	7.45	9.22	6.97	6.56	8.87	9.46	3.78
Ab	17.34	23.69	25.17	25.73	4.45	28.52	8.32	22.85	9.98	10.31	12.30	17.87	34.27	18.24	27.49	4.80	5.55	22.42
An	14.35	17.22	22.41	18.77	14.22	23.39	19.59	24.15	24.28	21.44	19.25	19.93	16.34	13.68	17.33	12.70	18.30	23.76
Ne	5.28	0.00	2.59	3.34	15.15	0.00	9.52	0.00	4.68	8.30	4.80	4.48	0.00	8.96	1.66	13.90	5.24	0.00
Di	*19.03*	*16.00*	*17.76*	*20.05*	*25.05*	*17.56*	*19.67*	*16.09*	*21.70*	*22.87*	*17.15*	*19.33*	*17.42*	*24.19*	*16.28*	*21.05*	*26.05*	*13.88*
En ..	6.30	4.71	5.30	5.51	7.93	6.02	6.92	4.56	8.24	8.02	5.78	6.29	5.10	7.12	4.86	7.06	8.88	4.17
Fs ..	2.89	3.11	3.36	4.34	4.22	2.44	2.53	3.32	2.09	2.96	2.49	3.07	3.41	4.69	3.09	3.10	3.67	2.60
Wt ..	9.84	8.19	9.09	10.20	12.89	9.11	10.23	8.20	11.37	11.89	8.88	9.97	8.91	12.38	8.34	10.90	13.50	7.11
Hy	*0.00*	*8.13*	*0.00*	*0.00*	*0.00*	*3.68*	*0.00*	*5.40*	*0.00*	*0.00*	*0.00*	*0.00*	*0.39*	*0.00*	*0.00*	*0.00*	*0.00*	*25.37*
Et ..	0.00	4.90	0.00	0.00	0.00	2.62	0.00	3.12	0.00	0.00	0.00	0.00	0.24	0.00	0.00	0.00	0.00	15.66
Ft ..	0.00	3.22	0.00	0.00	0.00	1.06	0.00	2.27	0.00	0.00	0.00	0.00	0.16	0.00	0.00	0.00	0.00	9.70
Ol	*29.05*	*15.28*	*16.21*	*14.43*	*22.91*	*6.11*	*19.39*	*13.57*	*20.29*	*17.87*	*21.04*	*19.04*	*9.48*	*17.23*	*20.20*	*21.67*	*20.67*	*0.00*
Fo ..	19.30	9.15	9.55	7.73	14.44	4.23	13.83	7.53	15.87	12.70	14.27	12.38	5.46	9.98	11.88	14.60	14.20	0.00
Fa ..	9.75	6.67	6.67	6.71	8.47	1.89	5.56	6.04	4.43	5.17	6.77	6.65	4.02	7.25	8.32	7.07	6.46	0.00
Mt	0.45	5.37	2.07	1.46	1.35	5.23	6.24	4.06	5.95	6.38	6.82	4.12	4.12	2.22	3.12	5.66	5.80	2.07
Il	3.46	4.18	3.80	4.08	4.81	4.27	4.37	3.04	4.37	4.37	4.18	4.08	6.10	4.60	4.50	5.32	4.75	3.38
Ap	1.26	1.40	1.97	1.00	1.04	1.04	3.62	1.21	1.47	1.87	2.04	1.63	1.47	2.32	1.00	2.84	1.97	0.43
$H_2O\pm$ ..	2.78	2.01	2.09	3.92	1.73	1.93	1.15	2.17	1.78	0.96	2.80	2.11	2.09	2.53	3.33	2.89	1.52	1.84
Total ..	101.33	99.73	100.87	99.22	99.22	99.24	101.09	100.22	100.41	100.69	99.84	100.04	100.90	100.94	101.47	99.70	99.31	99.18

TABLE 1—*Chemical Analysis and Molecular Norms—Tamar Tertiary Lavas—contd.*

Cation/Unit Cell. Oxygen	1	2	3	4	5	6	7	8	9	10	11	12	13	14	15	16	17	18
Si	29.53	28.61	29.04	28.66	26.94	29.14	26.36	28.98	26.57	26.88	26.36	27.79	30.01	28.34	29.02	25.28	26.42	31.00
Ti	0.86	1.02	0.91	0.98	1.19	1.02	1.08	0.73	1.07	1.08	1.03	1.00	1.46	1.12	1.09	1.33	1.18	0.81
Al	8.92	8.74	10.91	10.20	9.62	10.99	10.21	10.57	9.91	10.27	9.50	9.97	10.24	9.49	9.72	9.09	8.45	9.76
Fe^{+++}	0.14	1.72	0.65	0.46	0.44	1.64	2.02	1.29	1.91	2.06	2.21	1.32	1.30	0.71	0.99	1.86	1.89	0.65
Fe^{++}	5.24	5.99	4.45	4.74	5.66	3.36	4.79	5.00	4.14	4.79	5.22	4.84	4.44	5.31	5.34	5.66	5.47	4.42
Mn	0.13	0.11	0.09	0.08	0.07	0.11	0.05	0.10	0.09	0.05	0.12	0.09	0.09	0.13	0.10	0.13	0.11	0.09
Mg	12.72	8.38	6.86	6.01	10.67	5.29	9.94	6.73	11.42	9.74	9.78	8.82	4.76	7.89	7.98	10.55	10.97	7.13
Ca	5.61	5.43	6.49	6.02	6.47	6.25	7.28	6.21	7.42	7.40	6.23	6.42	5.46	6.62	5.29	6.37	7.62	5.45
Na	3.90	3.35	4.16	4.44	4.64	3.94	3.70	3.19	2.64	3.66	3.03	3.69	4.76	4.91	4.28	4.41	2.20	3.09
K	1.13	0.79	0.89	0.84	1.44	0.98	1.24	1.01	0.79	0.85	1.28	0.99	1.21	0.93	0.87	1.21	1.28	0.49
P	0.28	0.31	0.43	0.22	0.23	0.22	0.81	0.26	0.32	0.42	0.46	0.36	0.32	0.51	0.22	0.64	0.44	0.09

1. Olivine-basalt. Lower flow, east end of Greens Beach, Tamar Heads.
2. Olivine-basalt. Upper flow, above road cut, 70 ft level, Inspection Head, West Tamar.
3. Porphyritic olivine-basalt. West bank of East Arm, above 200 ft level, 1 mile NW. of Fourteen Mile Creek, East Tamar.
4. Coarse olivine-basalt. West bank of East Arm, H.E.C. pylon, 225 ft level, 1 mile NW. of Fourteen Mile Creek, East Tamar.
5. Coarse olivine-basalt. Picritic phase, west shore of East Arm, $\frac{3}{4}$ mile NW. of Fourteen Mile Creek, East Tamar.
6. Coarse olivine-basalt. Mesostasis rich-phase, west bank of East Arm, 150 ft level, $\frac{3}{4}$ mile NW. of Fourteen Mile Creek, East Tamar.
7. Olivine-basalt. Upper West Tamar Highway, $\frac{3}{4}$ mile N. of Muddy Creek.
8. Coarse olivine-basalt. Scarp top, above West Tamar Highway, S. of Atkinsons Creek, 1 mile due S. of Rosevears.
9. Pyroxene-olivine-basalt. North Esk, $1\frac{1}{4}$ miles N. of Corra Linn.
10. Olivine-basalt. Quarry, above 'Talisker' Farm, Rose Rivulet.
11. Olivine-basalt. $1\frac{1}{2}$ miles SE. of White Hills.
12. Average alkali olivine-basalt. Tamar Trough (average of analyses 1-11).
13. Pegmatite. In coarse olivine-basalt, plateau, $1\frac{1}{2}$ miles N. of Craigburn, East Tamar.
14. Nepheline-basanite. Fine grained phase, Deviot shore, West Tamar.
15. Nepheline-basanite. Coarse olivine-basalt phase, Deviot shore, West Tamar.
16. Olivine-nephelinite. East Arm Road–Batman Bridge Road Junction, N. of Spring Bay, East Tamar.
17. Limburgite. 'Duneiden' Farm, 2 miles ESE. of St Leonards.
18. Tholeiitic olivine-basalt. 7EX Hill, St Leonards.

Analyses 1, 3-6, 13-15, and 18, by X-ray fluorescence, with Na_2O and K_2O by flame photometry, and FeO by titration using the method of Reichen and Fahey (1962): F. L. Sutherland, analyst.

Analyses 7, 10, and 17, mainly by X-ray fluorescence, with Na_2O and K_2O by flame photometry: D.I. Groves and G. Sanders, analysts.

Analyses 2, 8, 9, 11 and 16, by Tasmanian Mines Department Laboratories, Launceston: J. Furst, analyst.

TABLE 2

Analyses of Pyroxenes and Spinel from pyroxene-olivine-basalt, Corra Linn and Blessington

Analysis	1 Augite-xenocryst core	2 Augite-xenocryst core	3 Augite-in reaction rim	4 Augite-new overgrowth	5 Spinel xenocryst	6 Clino-pyroxene-peridotite nodule
SiO_2	48.8	48.8	49.4	48.8	..	52.9
TiO_2	0.6	0.8	0.8	1.3	0.7	0.3
Al_2O_3 ..	9.2	10.2	6.9	6.6	64.9	7.3
Total FeO ..	5.7	6.4	6.2	6.8	16.4	2.0
MnO ..	0.4	0.4	0.4	0.4	..	0.2
MgO ..	17.0	15.0	16.1	14.6	18.4	16.6
CaO	17.9	18.4	19.6	20.2	..	19.0
Na_2O ..	0.9	1.0	0.4	0.4	..	1.4
K_2O	<0.01	<0.01	<0.03	<0.01	..	<0.01
Cr_2O_3 ..	..	..	..	..	0.2	..
Total ..	100.5	101.0	99.8	99.1	100.6	99.7

Microprobe analyses by courtesy of N. Gray and D. H. Green, Australian National University.
Analyses 1-5 from Corra Linn basalt, analysis 6 from Blessington basalt.

REFERENCES

BARTH, T. W. F., 1931—Mineralogical Petrography of Pacific Lavas. *Amer. J. Sci.* 125, pp. 377-405. *Ibid.*, 126, pp. 491-530.

BLACK, P. M., and BROTHERS, R. N., 1965—Olivine Nodules from Tokatoka, Northland. *N.Z.J. Geol. Geophys.*, **8**, 1, pp. 62-80.

BROTHERS, R. N., 1960—Olivine Nodules from New Zealand. *Rep. 21st Int. Geol. Cong.*, **13**, pp. 68-81.

BULTITUDE, R. J., and GREEN, D. H., 1968.—Experimental Study at High Presures on the Origin of Olivine Nephelinite and Olivine Melilite Nephelinite Magmas. *Earth Planet Sci. Letters*, 3, 4, pp. 325-337.

DEER, W. A., HOWIE, R. A., and ZUSSMAN, J., 1963—Rock Forming Minerals *Chain Silicates*. Vol. **2**. Longmans, London.

EDWARDS, A. B., 1939—Petrology of the Tertiary Older Volcanic Rocks of Victoria. *Proc. Roy. Soc. Vict.* 51, 1, pp. 73-98.

——————, 1941—The Crinanite Laccolith of Circular Head, Tasmania. *Proc. Roy. Soc. Vict.*, 53, 2 (N.S.) pp. 403-415.

EDWARDS, A. B., 1950—The Petrology of the Cainozoic Basaltic Rocks of Tasmania. *Proc. Roy. Soc. Vict.*, **62**, 1 (N.S.) pp. 97-120.

EMMONS, R. C., 1943—The Universal Stage. *Geol. Soc. Amer. Mem.* 8.

GEE, D., 1966—Table Cape Map Sheet. *Geol. Surv. Tasm.* 1-Mile Geol. Map Ser. No. 22.

GILL, E. D., and BANKS, M. R., 1956—Cainozoic History of the Mowbray Swamp and Other Areas of North-Western Tasmania. *Rec. Q. Vict. Mus.* N.S. 6.

GREEN, D. H. and RINGWOOD, A E., 1967—The Genesis of Basaltic Magmas. *Contr. Mineral and Petrol.*, 15, pp. 103-190.

GREEN, J., and POLDERVAART, A., 1958—Petrochemical Fields and Trends. *Geochim et Cosmoch Acta.*, **13**, pp. 87-122.

JOPLIN, G. A., 1963—Chemical Analyses of Australian Rocks. Pt. 1: Igneous and Metamorphic *Bull. Bur. Min. Resour. Aust.* 65.

——————, 1964—'A Petrography of Australian Igneous Rocks'. Angus and Robertson, Sydney.

KUNO, H., 1959—Origin of Cenozoic petrographic provinces of Japan and surrounding areas. *Bull. Volcan.* Ser. 2, 20, pp. 37-76.

————, 1960—High Alumina basalt. *J. Petrology* 1, pp. 121-145.

————, 1965—Fractionation Trends of Basalt Magmas in Lava Flows. *J. Petrology* 6, 2, pp. 302-321.

LONGMAN, M. J., 1966—Launceston *Explan. Rep. Geol. Surv.* Tas. 1-Mile Geol. Map. Ser. K'55-7-39.

MACDONALD, G. A., 1949—Hawaiian petrographic province. *Bull. Geol. Soc. Amer.*, 60, pp. 1541-1596.

————, and KATSURA, T., 1964—Chemical Composition of Hawaiian lavas. *J. Petrology* 5, pp. 82-133.

MUIR, E. D., and TILLEY, C. E., 1963—Contributions to the Petrology of the Hawaiian Basalts; II The Tholeiitic Basalts of Mauno Loa and Kilauea. *Amer. J. Sci.* 261, pp. 111-128.

MUNRO, M., 1966—The measurement of large optic axial angles with the Universal stage. *Min. Mag.* 35, pp. 763-769.

MURATA, K. J., 1960—A new method of plotting chemical analyses of basaltic rocks. *Amer. J. Sci.* 258A, pp. 247-252.

NOCKOLDS, S. R., 1954—Average Chemical Compositions of some Igneous Rocks. *Bull. Geol. Soc. Amer* 65, pp. 1007-1032.

REICHEN, L. A., and FAHEY, S., 1962—An Improved Method for the Determination of FeO in Rocks and Minerals, including Garnet. *U.S. Geol. Surv. Bull.* 144B.

RITTMANN, A., and EL-HINNAWI, E. E., 1961—The Application of the Zonal Method for the Distinction between Low- and High-Temperature Plagioclase Feldspars. *Schweiz. Miner. Petrogr. Mitt.*, 41, pp. 41-48.

SAGGERSON, E. P., and WILLIAMS, L. A. J., 1964—Ngurumanite from Southern Kenya and its Bearing on the Origin of Rocks in the Northern Tanganyika Alkaline District. *J. Petrology* 5, pp. 40-81.

SEARLE, E. J., 1960—Petrochemistry of the Auckland Basalts. *N.Z.J. Geol. Geophys.*, 3, 1, pp. 23-40.

————, 1961—The Petrology of the Auckland Basalts. *N.Z.J. Geol. Geophys.*, 4, 2, pp. 165-204.

————, 1962—Quartzose Xenoliths and Pyroxene Aggregates in the Auckland Basalts. *N.Z. J. Geol. Geophys.*, 5, 1, pp. 130-140.

SPRY, A. H., 1962—Igneous Activity in 'The Geology of Tasmania'. *J. Geol. Soc. Aust.*, 9, 2, pp. 255-284.

SUTHERLAND, F. L., 1966—The Tertiary Volcanics of the Tamar Valley, Northern Tasmania—A Preliminary Report. *Aust. J. Sci.*, 29, 4, pp. 114-115.

————, 1969a—A Comparison of the Cainozoic Volcanic Provinces of Victoria and Tasmania. *Proc. Roy. Sci. Vict.* (*in press*) 82, 2 (N.S.).

SUTHERLAND, F. L., 1969b—A Review of the Tasmanian Cainozoic Volcanic Province. *Palaeovolcanology Symposium. Geol. Soc. Aust.* (*in press*).

————, and CORBETT, K. D., 1967—The Tertiary Volcanic Rocks of the Far North-West Tasmania. *Proc. Roy. Soc. Tasm.*, 101, pp. 71-90.

TILLEY C. E., 1960—Differentiation of Hawaiian Basalts: Some Variants in Lava Suites of Dated Kilauean Eruptions. *J. Petrology* 1, pp. 47-55.

TURNER, F. J. and VERHOOGEN, J., 1951—'Igneous and Metamorphic Petrology'. McGraw Hill Book Co. Inc., N.Y.

WAGER, L. R., 1960—The Major Element Variation of the Layered Series of the Skaergaard Intrusion and a Re-estimation of the Average Composition of the Hidden Layered Series and of the Successive Residual Magmas. *J. Petrology* 1, pp. 364-498.

————, 1962—Igneous Cumulates from the 1902 Eruption of Soufrier, St Vincent *Bull. Vulcan.* 24, pp. 93-99.

WILKINSON, J. F. G., 1956a—The Olivines of a Differentiated Teschenite Sill near Gunnedah, New South Wales. *Geol. Mag.* 93, pp 414-455

———— 1956b—Clinopyroxenes of Alkali Olivine-Basalt Magma. *Amer. Min.* 41, pp. 724-743.

————, 1957—The Clinopyroxenes of a differentiated teschenite sill near Gunnedah, New South Wales. *Geol. Mag.* 94, pp. 123-134.

————, 1958—The Petrology of a differentiated teschenite sill near Gunnedah, New South Wales. *Amer. J. Sci.* 256, pp. 1-39.

WILSHIRE, H. G., 1967—The Prospect Alkaline Diabase—Picrite Intrusion. N.S.W. Australia. *J. Petrology* 8, pp. 97-163.

————, and BINNS, R A., 1961—Basic and Ultrabasic Xenoliths from Volcanic Rocks of N.S.W. *J. Petrology* 2, pp. 185-208.

WYLLIE, P. J., 1959—Discrepancies between optic axial angles of olivines over different bisectrices. *Amer. Min.* 44, p. 49.

YAGI, K., 1953—Petrochemical studies of the alkalic rocks of the Morotu District, Sakhalin. *Bull. Geol. Soc. Amer.* 64, pp. 769-809.

————, and ONUMA, K., 1967—The Join $CaMgSi_2O_6$ $CaTiAl_2O_6$ and its Bearing on the Titan Augites. *J. Fac. Sci. Hokkaido Univ. Ser. IV. Geol. & Min.* XIII, 4, pp. 463-483.

LIST OF PLATES

PLATE 1—Olivine-basalt. Lower flow, Inspection Head, lower Tamar. T.S. 369.
PLATE 2—Porphyritic olivine-basalt. Correlate of upper flow, lower Tamar? East Arm, middle Tamar. T.S. 281.
PLATE 3—Olivine-nephelinite. Spring Bay, Middle Tamar. T.S. 273.
PLATE 4—Nephelinite pegmatite. Spring Bay, middle Tamar. T.S. 284.
PLATE 5—Nepheline-basanite. Deviot, middle Tamar. T.S. 584.
PLATE 6—Coarse olivine-basalt (analcime bearing). Batman Bridge Road, East Arm, Middle Tamar. T.S. 232.
PLATE 7—Coarse olivine-basalt (picritic phase) East Arm foreshore, middle Tamar. T.S. 199.
PLATE 8—Coarse olivine-basalt (pegmatitic phase) Craigburn plateau, middle Tamar. T.S. 191.
PLATE 9—Olivine-basalt. Lower flow, Strathlyn, upper Tamar, T.S. 251.
PLATE 10—Augite xenocrysts, with reaction rims, and overgrowths of titaniferous augite, in olivine-basalt. 1¼ miles N. of Corra Linn, south Tamar. T.S. 562.
PLATE 11—Tholeiitic olivine-basalt. 7EX Hill, St Leonards, south Tamar. T.S. 173.
PLATE 12—Limburgite. 'Dunedin Farm', St Leonards, south Tamar. T.S. 207.

(All photomicrographs taken with uncrossed nicols. T.S. numbers refer to Tasmanian Museum thin section catalogue numbers)

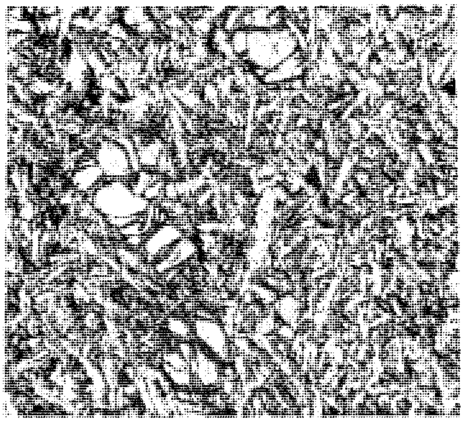

1

2

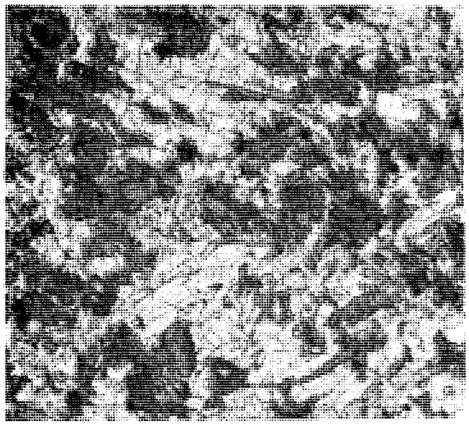

3

4

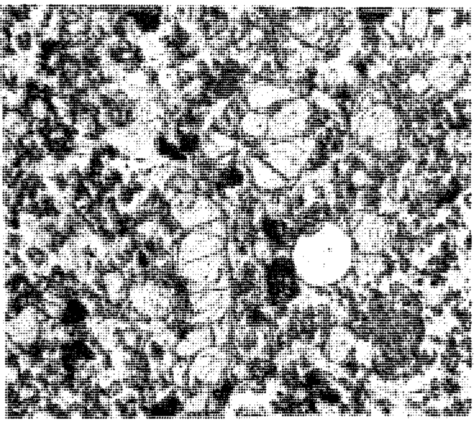

5

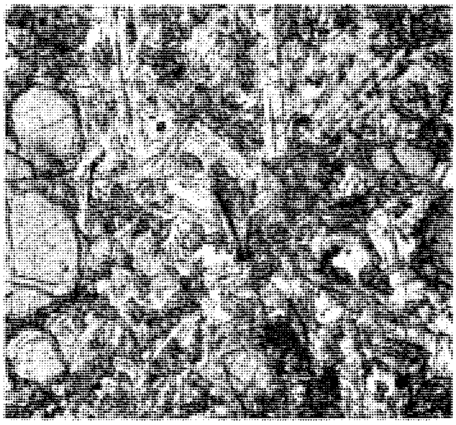

6

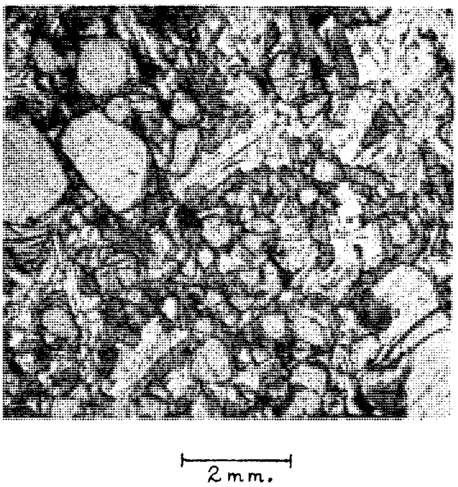

7

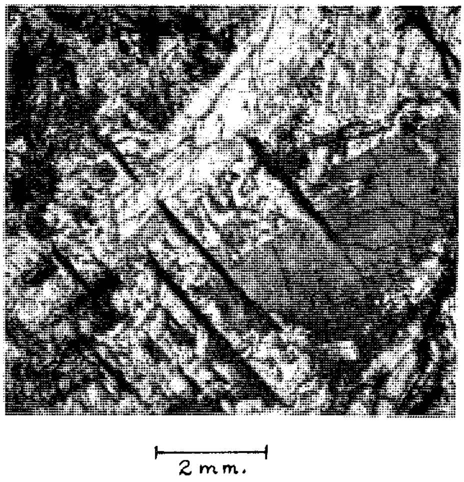

8

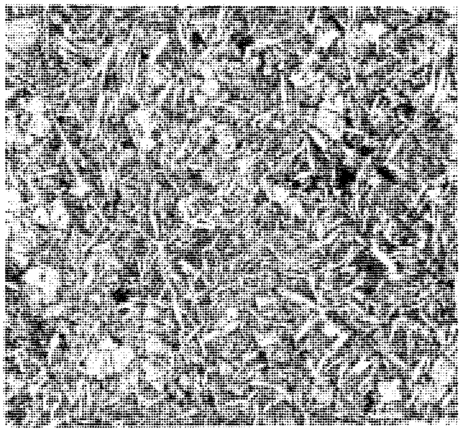

9

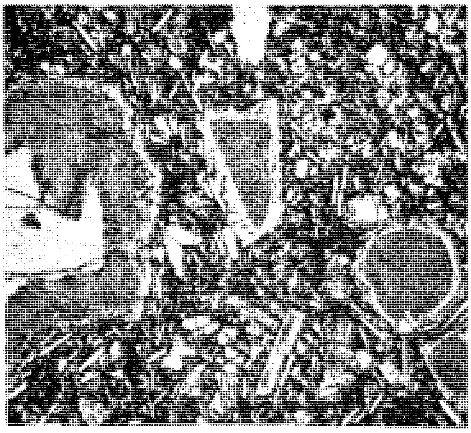

10

11

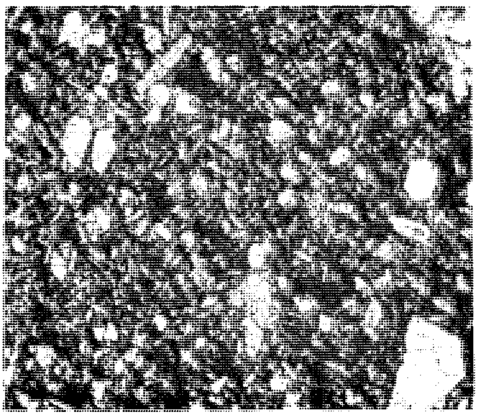

12